

Enhanced Harvesting of Red Photons in Nanowire Solar Cells: Evidence of Resonance Energy Transfer

Karthik Shankar,^{†,*} Xinjian Feng,[‡] and Craig A. Grimes^{†,*}

[†]Department of Electrical Engineering and [‡]The Materials Research Institute, The Pennsylvania State University, University Park, Pennsylvania 16802

ABSTRACT Modern excitonic solar cells efficiently harvest photons in the 350–650 nm spectral range; however, device efficiencies are typically limited by poor quantum yields for red and near-infrared photons. Using Förster-type resonance energy transfer from zinc phthalocyanine donor molecules to ruthenium polypyridine complex acceptors, we demonstrate a four-fold increase in quantum yields for red photons in dye-sensitized nanowire array solar cells. The dissolved donor and surface anchored acceptor molecules are not tethered to each other, through either a direct chemical bond or a covalent linker layer. The spatial confinement of the electrolyte imposed by the wire-to-wire spacing of the close-packed nanowire array architecture ensures that the distances between a significant fraction of donors and acceptors are within a Förster radius. The critical distance for energy transfer from an isolated donor chromophore to a self-assembled monolayer of acceptors on a plane follows the inverse fourth power instead of the inverse sixth power relation. Consequently, we observe near quantitative energy transfer efficiencies in our devices. Our results represent a new design paradigm in excitonic solar cells and show it is possible to more closely match the spectral response of the device to the AM 1.5 solar spectrum through use of electronic energy transfer.

KEYWORDS: energy transfer · dye-sensitized solar cells · photoelectrochemistry · titania · semiconductor · TiO₂ · rutile nanowires · nanowire arrays · arrays · light harvesting

Long-range Förster-type resonance energy transfer (FRET), also known as electronic energy transfer,¹ has recently experienced a resurgence of research interest. FRET-based quantum dot pH sensors have been made,² and electrical control of FRET in quantum dots has been demonstrated.³ FRET in organic molecules has been used to study conformational changes in DNA⁴ and to detect DNA with high sensitivity.⁵ It has also been used in solar concentrators⁶ and to improve quantum yields in organic light-emitting devices.^{7,8} Several ideas for FRET-based photovoltaic device enhancement have been proposed^{9–11} but, to the best of our knowledge, not been demonstrated, while in none of the proposed devices is the nanoscale architecture of the device integral to the use of FRET as it is in our configuration. Herein, we have sought to realize the high quantum yields achieved in thin film organic light-emitting

devices by energy transfer from a conductive host to a luminescent dopant in a low-cost hydrothermally processed photovoltaic device by exploiting the unique combination of a close-packed one-dimensional nanowire architecture and an efficient electron injecting acceptor infiltrated by a redox electrolyte containing soluble red-absorbing energy donors. Our work demonstrates that an enhancement in photovoltaic device performance is possible using long-range resonance energy transfer from a dissolved luminescent dopant confined in the interwire spaces of a nanowire array electrode to an acceptor species confined to the surface of the nanowires.

Photoconversion efficiencies greater than 10% have been reported for liquid junction dye-sensitized solar cells¹² and 5% for solid-state polymeric solar cells.¹³ It is generally agreed that new materials as well as advanced device concepts are necessary for further improvements in efficiencies. The use of FRET has been contemplated as an alternative mechanism for charge separation and a way to improve exciton harvesting by placing the exciton close to the heterojunction interface.¹⁴ In inorganic quantum-dot-based solar cells, the use of FRET to transfer the exciton generated in the quantum dot to a high mobility conducting channel, such as a nanowire or a quantum well, has been proposed as a way to bypass the traditional limitations of charge separation and transport.¹⁵ We report here on the use of FRET to boost the quantum yield for red photons at 675 to 680 nm by a factor of 4 for N-719 and a factor of 1.5 for black dye. The close-packed single crystal rutile nanowire array architecture¹⁶ developed by us is an essential ingredient of our strategy because it allows placement

*Address correspondence to cgrimes@enr.psu.edu.

Received for review January 30, 2009 and accepted March 13, 2009.

Published online March 20, 2009.
10.1021/nn900090x CCC: \$40.75

© 2009 American Chemical Society

of donor and acceptor molecules at distances comparable to a Förster radius. Figure 1 illustrates our idealized device configuration, with microscopy, spectral characteristics, and basic modeling indicating the nanowire array based device to be nearly ideal for FRET-based enhancement in photoconversion efficiency.

Figure 2 shows the molecular structures and optical properties of the dyes used in this study. We used phthalocyanines (traditionally acceptors) as energy donors and nonfluorescing ruthenium polypyridine complexes as acceptors. The bis(bipyridine) and terpyridine ruthenium complexes already have broad absorption in the visible region of the spectrum and excellent charge transfer characteristics, thus establishing a high baseline of light harvesting. Our choice of phthalocyanines was driven by three considerations: light absorption, solubility, and aggregation. Electronic transitions occurring in the 18π electronic structure of a phthalocyanine molecule result in intense visible absorption Q and ultraviolet Soret bands. For the purposes of this study, we were interested in utilizing the Q band to improve the harvesting of red photons. Zinc phthalocyanine (ZnPc) has good thermal stability and strong Q-band absorption at ca. 700 nm in solution form. However, ZnPc has low solubility in common organic solvents. Phthalocyanines also have a pronounced tendency to aggregate by forming $\pi-\pi$ stacking structures, which manifest themselves in a broader band absorption, blue-shifted with respect to the solution phase Q band. Aggregation is extremely negative for FRET-based devices since self-quenching of the phthalocyanine fluorescence can significantly reduce or eliminate resonance energy transfer. We chose zinc 2,9,16,23-tetra-*tert*-butyl-29*H*,31*H*-phthalocyanine (ZnPc-TTB), whose molecular structure is shown in Figure 2a, because the four tertiary butyl groups attached to the ZnPc core disrupt the formation of $\pi-\pi$ stacking structures thereby reducing aggregation and improving solubility in common organic solvents. Figure 2b presents the absorption and emission spectra of ZnPc-TTB, along with the absorption spectra of ruthenium polypyridine complex dyes. There is significant overlap between the emission spectrum of ZnPc-TTB and the absorption spectrum of N-719, while for the donor–acceptor pair of ZnPc-TTB and black dye, the emission spectrum of the donor is completely contained within the absorption spectrum of the acceptor.

RESULTS AND DISCUSSION

We observe in Figure 3a that the emission of ZnPc-TTB is dramatically quenched by dilute solutions of N-719 and black dye, a necessary condition for FRET. Figure 3b shows the Stern–Volmer plot of the fluorescence quenching of ZnPc-TTB by N-719. The quenching rate constant k_q is determined to be $4.40 \times 10^{12} \text{ M}^{-1} \text{ s}^{-1}$, a value comparable to those reported for similar FRET studies ($10^{11} - 10^{12} \text{ M}^{-1} \text{ s}^{-1}$) and an order of magnitude higher than diffusion-controlled quenching pro-

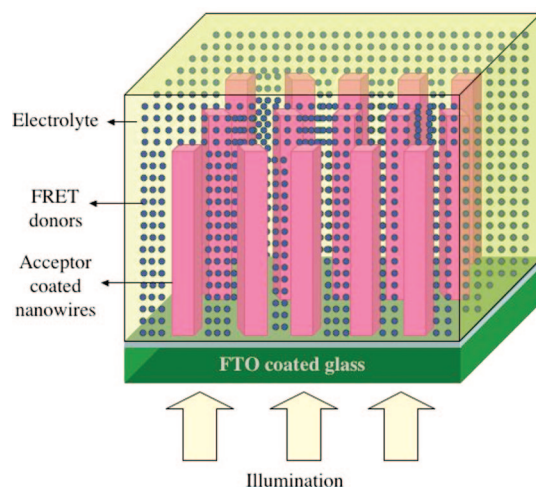


Figure 1. Concept of the FRET photovoltaic device. Depiction of the FRET-enhanced nanowire dye-sensitized solar cell.

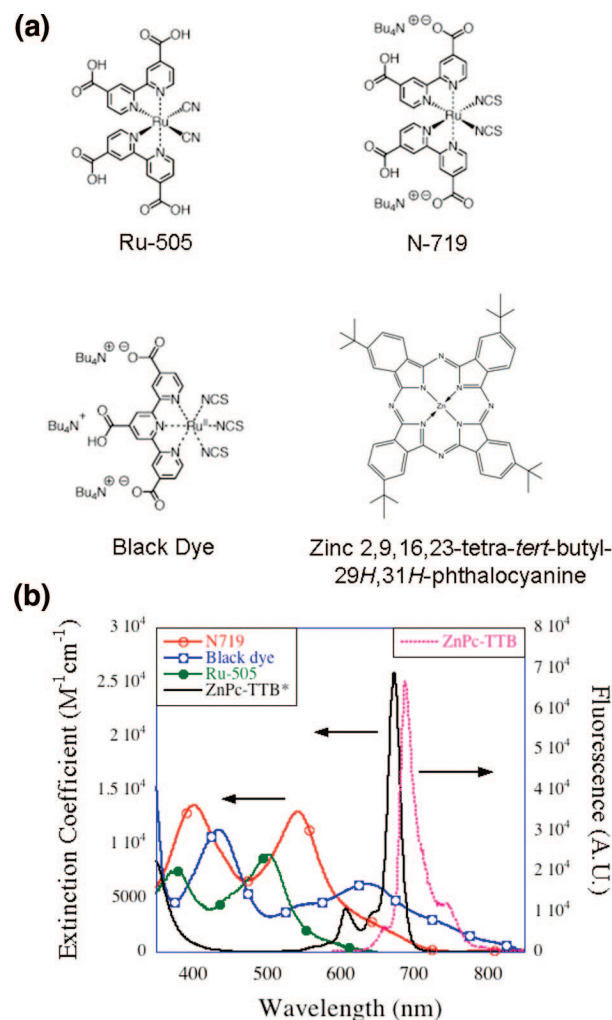


Figure 2. Dyes for resonance energy transfer. (a) Molecular structures of the dyes used in the study. (b) Absorption spectra of donor and acceptor dyes and emission spectrum of phthalocyanine donor. *For display purposes, 0.1 times the extinction coefficient of ZnPc-TTB is shown.

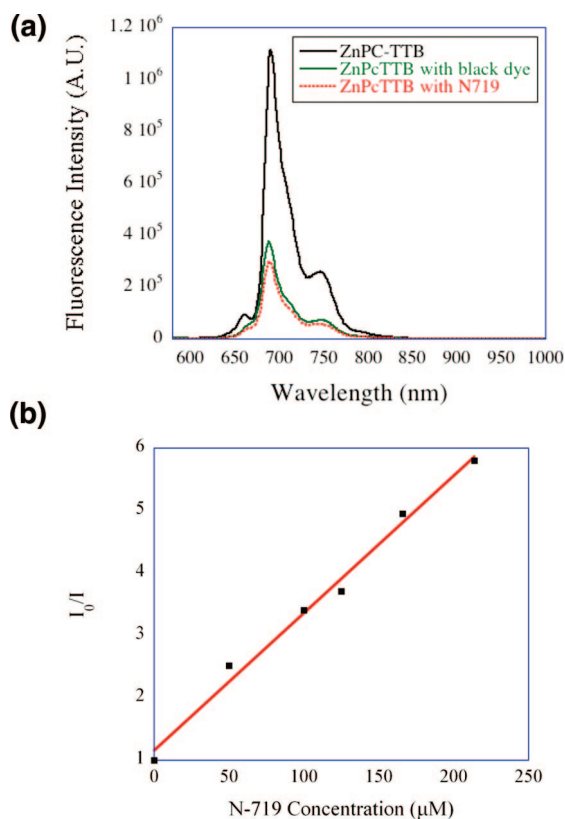


Figure 3. Energy transfer from donors to acceptors in solution. (a) Emission spectra of a 25 μM solution of ZnPC-TTB in THF under the following conditions: in the absence of acceptors (ZnPC-TTB), in the presence of 125 μM black dye, and in the presence of 125 μM N-719. (b) Stern–Volmer plot of the fluorescence quenching of ZnPC-TTB by N-719.

cesses,¹⁷ confirming that energy transfer from ZnPC donors to N-719 acceptors is the dominant mechanism of the fluorescence quenching. The efficiency of energy transfer is given by the relation¹

$$\varphi_{\text{ET}} = \frac{k_{\text{ET}}}{k_{\text{ET}} + \frac{1}{\tau_{\text{D}}} + k_{\text{w}}} \quad (1)$$

The rate of energy transfer from donor to acceptor is given by k_{ET} ; τ_{D} is the excited-state lifetime of the donor in the absence of the acceptor, and k_{w} is the effective rate of any other competing process. The rate of Förster energy transfer for two point dipoles separated a distance r is

$$k_{\text{ET}}(r) = \frac{1}{\tau_{\text{D}}} \left(\frac{R_0}{r} \right)^6 \quad (2)$$

R_0 is given by the well-known expression for the Förster radius:¹

$$R_0^6 = \frac{9000 \ln(10) \kappa^2 \Phi_{\text{D}}}{128 \pi^5 N_{\text{A}} n^4} \left[\int_0^{\infty} F_{\text{D}}(v) \varepsilon_{\text{A}}(v) v^{-4} dv \right] \quad (3)$$

The refractive index is given by n ; N_{A} is the Avogadro number, κ is the dipole orientation factor, and Φ_{D} is the

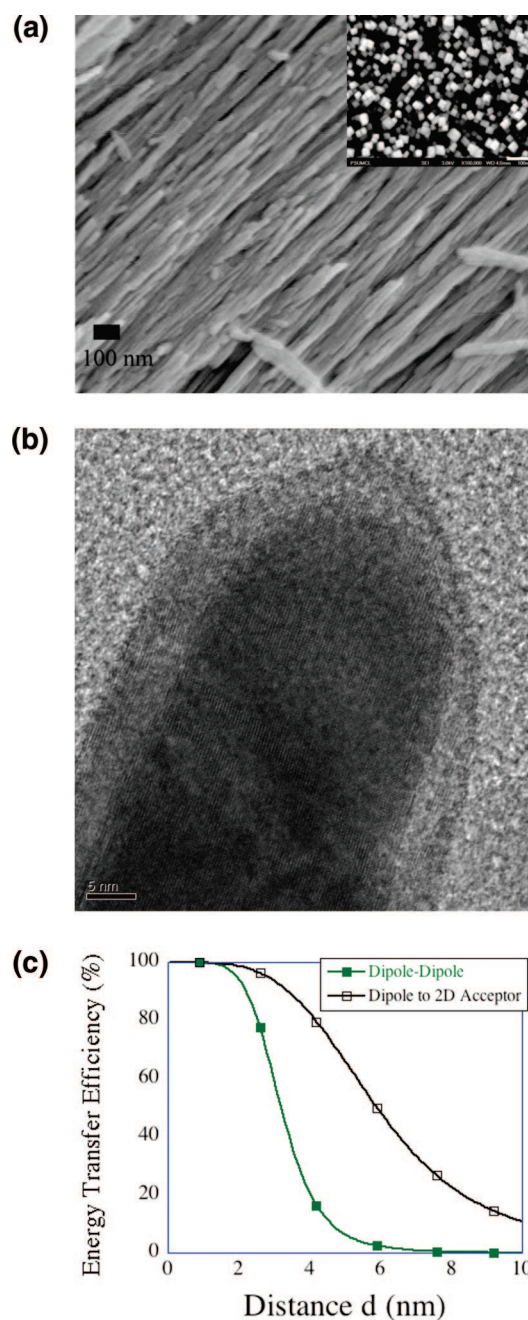


Figure 4. Characterization and modeling of FRET-enhanced nanowire solar cells. (a) Field emission scanning electron microscope cross section and (inset) top view of the rutile nanowire arrays. (b) High-resolution transmission electron microscope (HRTEM) image of a single crystal rutile nanowire. (c) Simulated effect of interwire spacing on the efficiency of energy transfer from ZnPC-TTB donors to isolated N-719 acceptors (dipole–dipole), and a close-packed monolayer of N-719 (dipole to 2D acceptor).

donor fluorescence quantum yield in the absence of acceptor. The terms within the square brackets constitute the spectral overlap integral J of the donor fluorescence intensity (normalized to unit area)¹⁸ and the absorption spectrum of the acceptor.

For our photoanode, we employ a self-organized vertically oriented array of single crystal rutile TiO_2 nanowires fabricated by a facile hydrothermal

TABLE 1. Critical Distances for Excitation Transfer from Dipole \rightarrow 2D Sheet and from Dipole \rightarrow Dipole for ZnPc-TTB Donors and Various Acceptors Used in This Study

acceptor	J ($\text{nm}^4 \text{M}^{-1} \text{cm}^{-1}$)	R_0 (nm)	$d_{0,\lambda_{\text{max}}}$ (nm)
N-719	1.81×10^{14}	3.2	4.9
black dye	8.65×10^{14}	4.1	3.9
Ru-505	1.47×10^{11}	0.98	

method.¹⁹ Figure 4a shows field emission scanning electron microscope (FESEM) images of a nanowire array, while Figure 4b shows a high-resolution transmission electron microscope (HRTEM) image of a rutile nanowire. We are able to grow 6–8 μm long extremely close-packed nanowire arrays with an interwire spacing of 5–10 nm as inferred from cross-sectional FESEM images. A key requirement for FRET is that the physical separation of the donor and acceptor species be close to the Förster radius for the donor–acceptor system. In our device configuration, the acceptor dye molecule is anchored to the surface of the nanowires. Due to the confinement of the liquid electrolyte in the interwire spaces of the electrode, a large number of donor dye molecules dissolved in solution are effectively within a Förster radius of the acceptor molecules, thus facilitating energy transfer between donor and acceptor molecules. However, energy transfer in our device architecture of solution-based donors and surface-confined acceptors is, we believe, better represented by a system consisting of energy transfer from a donor chromophore to a two-dimensional sheet of acceptors at a distance d . For this geometry, Kuhn¹⁹ showed that the rate of energy transfer follows the inverse fourth power of the interchromophoric distance:

$$k_{\text{ET}}(d) \propto \frac{1}{\tau_{\text{D}}} \left(\frac{d_0}{d} \right)^4 \quad (4)$$

where the critical distance d_0 is given by

$$d_0 = \left(\frac{\lambda_s}{4\pi n} \right) \left(\frac{9A_s \Phi_{\text{D}}}{2} \right)^{\frac{1}{4}} \quad (5)$$

λ_s is the wavelength of the luminescence maximum and A_s is the absorption given by

$$A_s = \left[\int_0^{\infty} F_{\text{D}}(\nu) A(\nu) \left(\frac{\nu_s}{\nu} \right)^4 d\nu \right] \quad (6)$$

Figure 4c is a plot of the calculated donor–dipole to acceptor–dipole and donor to a 2-D sheet of acceptors energy transfer efficiencies. The plot clearly shows that energy transfer efficiencies are enhanced when the acceptors are organized in a two-dimensional close-packed monolayer. Our estimates for the overlap integral J , the Förster radii R_0 , and the critical distance d_0 for the ZnPc-TTB donors and various acceptors used in this study are provided in Table 1. Please see Supporting Information for values of the constants used in esti-

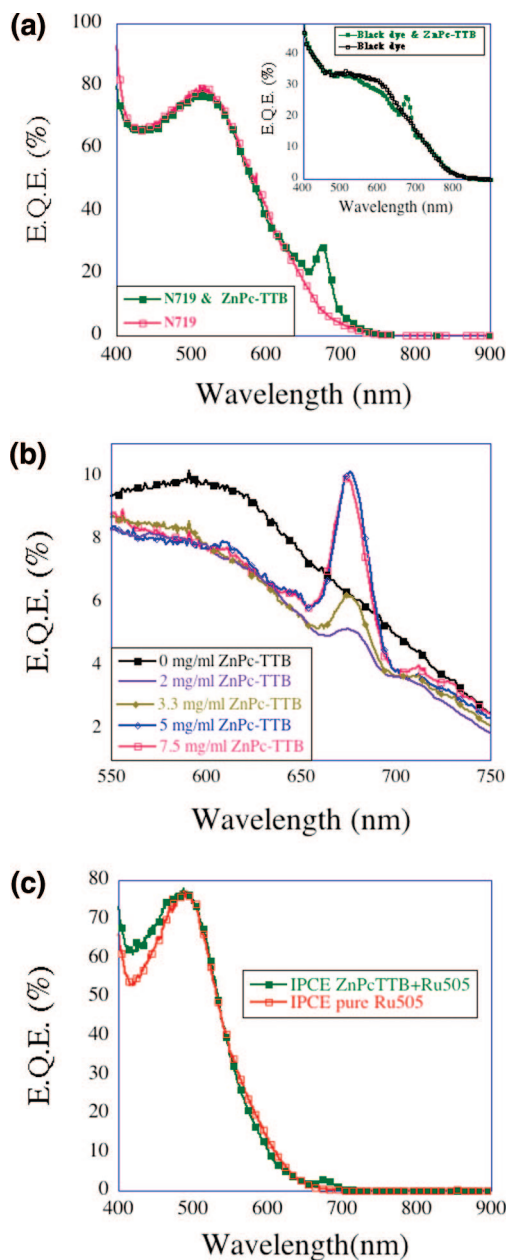


Figure 5. External quantum yields of FRET-enhanced nanowire solar cells. (a) Action spectrum of nanowire solar cell comprising N-719-coated rutile as acceptors, with and without ZnPc-TTB molecules in electrolyte as the donors. Inset shows action spectrum for black-dye-coated rutile acceptors with and without ZnPc-TTB donors. Ten percent of data points is shown. **(b)** Effect of donor concentration on the external quantum yield of red photons in black-dye-sensitized low surface area nanowire solar cells. Ten percent of data points is shown. **(c)** Action spectrum of nanowire solar cell comprising Ru-505-coated rutile as acceptors, with and without ZnPc-TTB molecules in electrolyte as the donors. Ten percent of data points is shown.

mating the spectral overlap integral and for a more detailed treatment of the effect of the nanowire array geometry.

In our device configuration, ZnPc-TTB molecules were introduced directly into the tri-iodide redox electrolyte at a (high) concentration of 1–5 mg/mL. As seen in Figure 5a, a dramatic increase in the quantum yield

for red photons in the spectral region of 670–690 nm was immediately observed, over and above the quantum yields exhibited by N-719 and black-dye-sensitized nanowire solar cells. N-719 dye forms a nonagglomerated monolayer.²⁰ Since black dye agglomerates, coadsorption of deoxycholic acid was employed to form the black dye coating and reduce agglomeration.²¹ The consequent dilution of black dye in the monolayer reduced the concentration of acceptors available for energy transfer and resulted in lower critical distance and lower energy transfer efficiencies for black dye relative to N-719 despite the higher spectral overlap of black dye absorption with the emission spectrum of ZnPc.

We explored the possibility of mechanisms other than FRET that could explain the observed results. One possibility is the interdigitation of phthalocyanines into the basal dye monolayer, in effect constituting a mixed monolayer of ruthenium dye and phthalocyanine. The concentration of phthalocyanines used by us were already in excess of the dye concentrations required to form a monolayer; therefore, a further increase in dye concentration should not impact quantum yields for red photons if a mixed monolayer had formed. We therefore studied effects of phthalocyanine concentration in the electrolyte, with results shown in Figure 5b. Since black dye has significant absorption in the spectral region of interest, a low surface area rutile nanowire array electrode was used for the study to observe the effect of the zinc phthalocyanine induced effect in isolation. Increasing the ZnPc-TTB concentration in the electrolyte increased the quantum yields for red photons. This is in agreement with what would be expected from a device employing FRET. As the concentration of FRET donors is increased, the likelihood of a spatially confined donor finding a surface-anchored acceptor increases, accounting for the observed result. Furthermore, when the ZnPc-TTB bearing electrolyte was removed and plain tri-iodide redox electrolyte was substituted in its place, the quantum yields for red photons dropped back to the basal levels observed for N-719 and black-dye-sensitized electrodes, respectively.

To examine the possibility of electron transfer instead of excitation transfer to the monolayer, we used Ru-505 as our basal dye sensitizer anchored to the surface of the nanowires. One defining characteristic enabling FRET is spectral overlap between donor and acceptor. In the absence of such overlap, transfer of red photon-generated excitons will not occur. Ru-505 is similar in structure to N-719, but the isothiocyanato (SCN) groups of N-719 are replaced by cyano (CN) groups in Ru-505, due to which the absorption of Ru-505 extends only to *ca.* 650 nm instead of *ca.* 750 nm for N-719 and *ca.* 920 nm for black dye. When a dye-sensitized solar cell using Ru-505-sensitized TiO₂ nanowire array electrode and ZnPC-TTB bearing tri-iodide redox electrolyte was constructed, the excess quantum yields for red photons were diminished to a small frac-

tion of those observed for N-719 and black dye (see Figure 5c). These results strongly support our contention that Förster resonance energy transfer is responsible for the observed enhancement in quantum yield for red photons.

Resonance energy transfer of excitons generated in ZnPc-TTB molecules from red photons to surface-bound N-719 dye results in a four-fold enhancement of quantum yield at 675 to 680 nm. Since the extinction coefficient of ZnPc-TTB molecules in the spectral region of 670–690 nm is far greater than that of N-719, we believe the entire quantum yield of ~28% at the donor absorption maximum is attributable to FRET and is close to the measured fluorescence quantum yield of ZnPc-TTB in solution.²² At the high concentrations used, zinc phthalocyanine forms multimolecular aggregates with a reduced quantum yield due to concentration quenching. A self-sieving effect of the nanowires admitting only monomeric and dimeric forms into the interwire spaces may account for the nearly quantitative efficiency of energy transfer from ZnPC-TTB in solution to surface-anchored N-719 and black dye molecules, a hypothesis supported by the saturation of the external quantum yields for red photons at values close to the fluorescence quantum yield of the donor (please see Supporting Information for a discussion of possible self-sieving). Comparison of these results with the simulation presented in Figure 4c indicates the importance of the closely spaced nanowire array architecture¹⁶ in achieving high energy transfer efficiencies.

Most researchers in this field agree that the greatest room for further improvement in efficiencies lies in better utilization of red and infrared photons, which are poorly utilized even by today's state-of-the-art dye-sensitized solar cells. Two approaches have traditionally been explored toward improving the utilization of red and infrared photons. The first approach consists of using the same bis(bipyridine) and terpyridine ruthenium complexes that were used in the early high efficiency dye-sensitized solar cells but modifying the architecture of the TiO₂ film to make it more ordered to improve charge collection and enhance external quantum yields for the red photons already absorbed.^{23,24} Low-dimensional architectures, such as vertically oriented nanowire and nanotube arrays, have already demonstrated superior charge collection efficiencies in DSCs.^{24,25} The second approach consists of using new dyes with enhanced absorption in the red and infrared regions of the solar spectrum, either in isolation or in conjunction with existing Ru-based dyes in dye cocktails. Many dyes have been developed and tested for this purpose, yet no dye with significant absorption over 750 nm has functioned properly.²⁶ There is some evidence that several candidate molecular systems for red and near-IR light harvesting act to promote recombination when anchored to the TiO₂ surface, in turn de-

grading the performance of the dye-sensitized solar cells which employ them.²⁵

Our results demonstrate that high external quantum efficiencies can be obtained for red photons by employing high surface area nanowire arrays and donor chromophores with high fluorescence quantum yields. We employ FRET in dye-sensitized solar cells to bypass three common limitations: (i) the poor charge transfer properties of dyes absorbing in the red and near-infrared regions of the solar spectrum; (ii) the poor spectral match of dyes that do have good charge transfer properties with the solar spectrum; and (iii) the necessity of energy level matching of the component dyes/organic semiconductors for exciton splitting in dye cascades and bilayer devices. Factor (iii) follows from the fact that as long as the conditions for efficient resonance energy transfer, namely, a high fluorescent quantum

yield of the donor, freely rotating chromophores, large spectral overlap of the donor fluorescence spectrum with the absorption spectrum of the acceptor dye, and donor–acceptor distances close to the critical distance (d_0 or R_0), are met, resonance energy transfer will occur irrespective of whether the HOMO–LUMO levels of the dye pair are matched or not. The prevalence of energy transfer in photosynthetic processes occurring in nature attests to the robustness of the process. Conventional nanoenabled devices utilize the large surface area of nanostructured electrodes to anchor dyes and obtain light absorption that is subsequently converted into electrical signals for sensing, catalysis, electrochromism, photovoltaics, etc. In this study, we present a new paradigm for nanoenabled devices by showing that the confined volume element of nanostructured electrodes may be used, as well.

METHODS

Synthesis of TiO₂ Nanowire Arrays. TiO₂ nanowire arrays were synthesized on clean FTO-coated glass (TEC-8, 8 Ω per square) substrates by nonpolar solvent/hydrophilic substrate interfacial reaction under mild hydrothermal conditions. A 20 nm thin compact TiO₂ layer was first formed on FTO substrates by immersion in a 0.1 M TiCl₄ solution at 80 °C for 0.5 h and then heating in air at 500 °C for 0.5 h. The substrates were then loaded into a sealed Teflon reactor (23 mL), containing 10 mL of toluene, 0.3 mL of tetrabutyltitanate, 1 mL of titanium tetrachloride (1 M in toluene), and 1 mL of hydrochloric acid (37 wt %). The hydrothermal reaction was carried out at a temperature of 180 °C for 8 h.

Dye Sensitization and Solar Cell Construction. N-719, black dye, and Ru-505 were obtained from Solaronix, Inc. (Switzerland) and used as received. ZnPc-TTB was purchased from Sigma Aldrich, Inc. and used as received. The nanowire electrodes were laminated by a 25 μm thick SX-1170 spacer (Solaronix Inc., Switzerland) with a central window, which constituted the active area of the device. The active area was measured using a calibrated optical microscope and determined to be 0.1–0.2 cm² for individual devices. Nanowire array electrodes were sensitized by ruthenium polypyridinium dyes by overnight immersion in a 1:1 solution of the dyes in ethanol and acetonitrile of concentration 5×10^{-4} M. For reference devices, the redox electrolyte contained lithium iodide (LiI, 0.1 M), diiodine (I₂, 0.02 M), 4-*tert*-butylpyridine (TBP, 0.5 M), butyl methyl imidazolium iodide (BMII, 0.6 M), and guanidinium thiocyanate (GuNCS, 0.1 M) in a mixture of acetonitrile, tetrahydrofuran, and methoxypropionitrile (v/v/v 4/5/1). For FRET devices, the above redox electrolyte also contained 1–10 mg mL⁻¹ ZnPc-TTB. A conductive glass slide sputter-coated with 100 nm of Pt was used as the counter electrode.

Morphological and Optical Characterization. The morphology, crystal structure, optical absorption, and photoluminescence of samples were characterized with FESEM (JEOL 6700F), HRTEM (Phillips 420 T), UV–vis–NIR spectrophotometer (Perkin-Elmer λ-950) and fluorescence spectrophotometer (Photon Technology Instruments), respectively.

Electrical Measurements of Nanowire Arrays. For collection of device action spectra, illumination was provided by a 300 W Oriol Solar Simulator. An Oriol Cornerstone 130 monochromator was used, and the intensity was calibrated using a Newport-Oriel photodetector (single crystalline silicon) and power meter. For longer wavelengths ($\lambda > 650$ nm), a band-stop optical filter with a 550 nm cutoff was used to eliminate the influence of second harmonics.

Acknowledgment. Support of this work through the Department of Energy, Grant Number DE-FG36-08GO18074, is gratefully acknowledged. The authors thank Carl Myers, Amit Vaish, and Prof. Mary Elizabeth Williams of Penn State University, Department of Chemistry, for assistance in collecting the fluorescence data, and Oomman K. Varghese for assistance in collecting HRTEM data.

Note added after ASAP publication: In the original version of this paper, published on the Web on March 20, 2009, an author's name was misspelled. The corrected version was reposted on the Web on March 30, 2009.

Supporting Information Available: Values of constants used to estimate spectral overlap integrals and Förster radii are provided along with a more elaborate discussion of possible self-sieving of donor molecules in the interwire voids. There is also a discussion on the effect of spatial restrictions on energy transfer in the most general case, and the differences between donors interacting with isolated acceptors and ensembles of acceptors. This material is available free of charge via the Internet at <http://pubs.acs.org>.

REFERENCES AND NOTES

- Föster, T. 10th Spiers Memorial Lecture: Transfer Mechanisms of Electronic Excitation. *Discuss. Faraday Soc.* **1959**, *27*, 7–17.
- Snee, P. T.; Somers, R. C.; Nair, G.; Zimmer, J. P.; Bawendi, M. G.; Nocera, D. G. A Ratiometric CdSe/ZnS Nanocrystal pH Sensor. *J. Am. Chem. Soc.* **2006**, *128*, 13320–13321.
- Becker, K.; Lupton, J. M.; Muller, J.; Rogach, A. L.; Talapin, D. V.; Weller, H.; Feldmann, J. Electrical Control of Förster Energy Transfer. *Nat. Mater.* **2006**, *5*, 777–781.
- Clegg, R. M.; Murchie, A. I. H.; Zechel, A.; Lilley, D. M. J. Observing the Helical Geometry of Double-Stranded DNA in Solution by Fluorescence Resonance Energy-Transfer. *Proc. Natl. Acad. Sci. U.S.A.* **1993**, *90*, 2994–2998.
- Zhang, C. Y.; Yeh, H. C.; Kuroki, M. T.; Wang, T. H. Single-Quantum-Dot-Based DNA Nanosensor. *Nat. Mater.* **2005**, *4*, 826–831.
- Currie, M. J.; Mapel, J. K.; Heide, T. D.; Goffri, S.; Baldo, M. A. High-Efficiency Organic Solar Concentrators for Photovoltaics. *Science* **2008**, *321*, 226–228.
- Baldo, M. A.; O'Brien, D. F.; You, Y.; Shoustikov, A.; Sibley, S.; Thompson, M. E.; Forrest, S. R. Highly Efficient Phosphorescent Emission from Organic Electroluminescent Devices. *Nature* **1998**, *395*, 151–154.

8. Chin, P. T. K.; Hikmet, R. A. M.; Janssen, R. A. J. Energy Transfer in Hybrid Quantum Dot Light-Emitting Diodes. *J. Appl. Phys.* **2008**, *104*, 013108.
9. Hasselman, G. M.; Watson, D. F.; Stromberg, J. R.; Bocian, D. F.; Holten, D.; Lindsey, J. S.; Meyer, G. J. Theoretical Solar-to-Electrical Energy-Conversion Efficiencies of Perylene-Porphyrin Light-Harvesting Arrays. *J. Phys. Chem. B* **2006**, *110*, 25430–25440.
10. Hardin, B. E.; Hoke, E. T.; Peters, C.; Geiger, T.; Nuesch, F.; Gratzel, M.; Nazeeruddin, M. K.; McGehee, M. D. In *Using Long Range Forster Energy Transfer to Increase Light Absorption in Dye Sensitized Solar Cells*; 2008 Materials Research Society Fall Meeting, Boston, MA, 2008.
11. Koeppe, R.; Bossart, O.; Calzaferri, G.; Sariciftci, N. S. Advanced Photon-Harvesting Concepts for Low-Energy Gap Organic Solar Cells. *Sol. Energy Mater. Sol. Cells* **2007**, *91*, 986–995.
12. Oregan, B.; Gratzel, M. A Low-Cost, High-Efficiency Solar-Cell Based on Dye-Sensitized Colloidal TiO₂ Films. *Nature* **1991**, *353*, 737–740.
13. Yu, G.; Gao, J.; Hummelen, J. C.; Wudl, F.; Heeger, A. J. Polymer Photovoltaic Cells: Enhanced Efficiencies via a Network of Internal Donor–Acceptor Heterojunctions. *Science* **1995**, *270*, 1789–1791.
14. Liu, Y. X.; Summers, M. A.; Scully, S. R.; McGehee, M. D. Resonance Energy Transfer From Organic Chromophores to Fullerene Molecules. *J. Appl. Phys.* **2006**, *99*, 093521.
15. Lu, S.; Madhukar, A. Nonradiative Resonant Excitation Transfer from Nanocrystal Quantum Dots to Adjacent Quantum Channels. *Nano Lett.* **2007**, *7*, 3443–3451.
16. Feng, X. J.; Shankar, K.; Varghese, O. K.; Paulose, M.; Latempa, T. J.; Grimes, C. A. Vertically Aligned Single Crystal TiO₂ Nanowire Arrays Grown Directly on Transparent Conducting Oxide Coated Glass: Synthesis Details and Applications. *Nano Lett.* **2008**, *8*, 3781–3786.
17. Misra, V.; Mishra, H. Effect of Polymer Microenvironment on Excitation Energy Migration and Transfer. *J. Phys. Chem. B* **2008**, *112*, 4213–4222.
18. Braslavsky, S. E.; Fron, E.; Rodriguez, H. B.; Roman, E. S.; Scholes, G. D.; Schweitzer, G.; Valeur, B.; Wirz, J. Pitfalls and Limitations in the Practical Use of Forster's Theory of Resonance Energy Transfer. *Photochem. Photobiol. Sci.* **2008**, *7*, 1444–1448.
19. Kuhn, H. Classical Aspects of Energy Transfer in Molecular Systems. *J. Chem. Phys.* **1970**, *53*, 101–108.
20. Wenger, B.; Gratzel, M.; Moser, J.-E. Rationale for Kinetic Heterogeneity of Ultrafast Light-Induced Electron Transfer from Ru(II) Complex Sensitizers to Nanocrystalline TiO₂. *J. Am. Chem. Soc.* **2005**, *127*, 12150–12151.
21. Ikeda, M.; Koide, N.; Han, L.; Sasahara, A.; Onishi, H. Scanning Tunneling Microscopy Study of Black Dye and Deoxycholic Acid Adsorbed on a Rutile TiO₂(110). *Langmuir* **2008**, *24*, 8056–8060.
22. Fernandez, D. A.; Awruch, J.; Dicoelio, L. E. Photophysical and Aggregation Studies of *t*-Butyl-Substituted Zn Phthalocyanines. *Photochem. Photobiol.* **1996**, *63*, 784–792.
23. Law, M.; Greene, L. E.; Johnson, J. C.; Saykally, R.; Yang, P. D. Nanowire Dye-Sensitized Solar Cells. *Nat. Mater.* **2005**, *4*, 455–459.
24. Zhu, K.; Neale, N. R.; Miedaner, A.; Frank, A. J. Enhanced Charge-Collection Efficiencies and Light Scattering in Dye-Sensitized Solar Cells using Oriented TiO₂ Nanotube Arrays. *Nano Lett.* **2007**, *7*, 69–74.
25. Mor, G. K.; Shankar, K.; Paulose, M.; Varghese, O. K.; Grimes, C. A. Use of Highly-Ordered TiO₂ Nanotube Arrays in Dye-Sensitized Solar Cells. *Nano Lett.* **2006**, *6*, 215–218.
26. O'Regan, B. C.; Lopez-Duarte, I.; Martinez-Diaz, M. V.; Forneli, A.; Alberio, J.; Morandeira, A.; Palomares, E.; Torres, T.; Durrant, J. R. Catalysis of Recombination and its Limitation on Open Circuit Voltage for Dye Sensitized Photovoltaic Cells Using Phthalocyanine Dyes. *J. Am. Chem. Soc.* **2008**, *130*, 2906–2907.